THE FINITE DIFFERENCE TIME DOMAIN METHOD FOR THE STUDY OF TWO-DIMENSIONAL ACOUSTIC AND ELASTIC BAND GAP MATERIALS

M. KAFESAKI[1], M. M. SIGALAS[1,2] AND N. GARCIA[1]
[1] *Laboratorio de Física de Sistemas Pequeños y Nanotecnología, Consejo Superior de Investigaciones Científicas, Serrano 144, 28006 Madrid, Spain.*
[2] *Agilent Laboratories, 3500 Deer Creek Rd., Palo Alto, CA 94304.*

Abstract. The finite difference time domain (FDTD) method has been proved recently an excellent tool for the study of classical wave propagation in periodic and random composite systems. Here we present in detail the method as it is applied in the case of *acoustic* and *elastic* wave propagation in *two-dimensional* composites. Also, we present some representative results of the method and we discuss its advantages.

1. Introduction

The propagation of acoustic (AC) and elastic (EL) waves in periodic media has been recently a problem of considerable interest [1–16]. This interest stems mainly from the fact that acoustic and elastic periodic media (phononic crystals) were found to exhibit, in a lot of cases, wide spectral gaps in their spectrum, gaps much lager than those observed in photonic crystals. This possibility of creating large gaps, which is given mainly by the variety of parameters controlling the AC and EL wave propagation in a composite system (densities, velocities), makes them very useful for the study of general question related with the wave propagation, such as the disorder induced localization of the waves. Additional reasons for the interest on the AC and EL wave propagation study are a) the possible applications of the AC and EL band gap materials (e.g. in filter and transducer technology); b) the rich physics of the AC and EL waves which stems from the variety of parameters controlling their propagation, the full vector character of the elastic waves and their scattering induced mode conversion (transformation of longitudinal wave to transverse and vice versa); and c) the ease in the fabrication of the AC and EL band gap structures. This ease is due to the fact that the characteristic structure lengths for gaps in the ultrasound regime are of the order of mm.

Among the methods which have been developed for the study of the AC and EL wave propagation in *periodic composites* the most widely used is the so called Plane Wave (PW) method [2–11]. PW is based on the expansion of the periodic coefficients in the wave equation and the periodic field amplitude in Fourier sums. The method, which can calculate very easily the band structure of infinite periodic systems and (in combination with a supercell scheme) in systems with isolated defects, has been used in most of the existing theoretical studies on AC and EL wave propagation. PW, however, presents some inefficiencies in the study of propagation in composites consisting of components with different phase (fluids in solids or solids in fluids) or composites with strong contrast in the elastic parameters of their components (the finite Fourier sums that approximate the elastic parameters in these composites do not succeed to describe functions with large discontinuities). Recently, a multiple scattering (MS) method [17] based in the electronic Korringa-Kohn-Rostoker theory came to cover some of the inefficiencies of the PW. MS method can calculate the band structure of infinite periodic systems and also the transmission of waves through small samples of a periodic or random composite. The method however has been applied until now [17, 16] only in fluid composites because, due to its heavy formalism, it is not easy to be extended to the case of full vector waves. Thus, for the study of the full elastic wave propagation in small finite samples the existing methods present certain inefficiencies, something that brings the necessity for a new method.

The FDTD method which we present here is based on the discretization of the full elastic time dependent wave equation through a finite difference scheme. Both the time and the space derivatives are approximated by finite differences and the field at a given time point is calculated through the field at the previous points. Thus one can obtain the field as a function of time at any point of a slab. The frequency dependence of the field is obtained by fast Fourier transform of the time results.

The FDTD method, while is well known in the acoustics community [18, 19, 20] and the seismology, had not been applied until recently in the study of the phononic crystals. Here the most important advantages of the method are that: a) it can give the field at any point inside and outside a sample, every time; b) it can give the field in both frequency and time domain; c) the FDTD results can be directly compared with the experiments since the method calculates the transmission through finite samples; d) it can be applied in systems with arbitrary material combination (e.g. solids in fluids or fluids in solids); e) it can be applied in periodic systems as well as in systems with arbitrary configuration of the scatterers, giving thus the possibility to study defect states, waveguides, random systems etc.

These important advantages of the method have been already exploited extensively in the field of EM wave band gap materials (photonic crystals) [21–25]. For AC and EL waves the study through the FDTD is still in the beginning [12, 26] while there is the lack of an extensive presentation of the method.

In what follows we present first the FDTD method as it is applied in two-dimensional (2D) systems, i.e. systems consisted of cylinders embedded in a homogeneous host. Then we present some characteristic FDTD results concerning propagation in a) periodic systems (in comparison with experimental and PW results), b) systems with isolated defects and c) systems with linear defects which can act as waveguides for waves with frequency in the regime of the gap.

2. Method

The starting point for the FDTD method is the elastic wave equation in isotropic inhomogeneous media [27],

$$\frac{\partial^2 u_i}{\partial t^2} = \frac{1}{\rho}\frac{\partial T_{ij}}{\partial x_j}, \tag{1}$$

where $T_{ij} = \lambda(\mathbf{r})u_{ll}\delta_{ij} + 2\mu(\mathbf{r})u_{ij}$ and $u_{ij} = (\partial u_i/\partial x_j + \partial u_j/\partial x_i)/2$ (in cartesian coordinates). In the above expressions u_i is the ith component of the displacement vector $\mathbf{u}(\mathbf{r})$, T_{ij} is the stress tensor and u_{ij} the strain tensor. Also $\lambda(\mathbf{r})$ and $\mu(\mathbf{r})$ are the so-called Lamé coefficients of the medium [27] and $\rho(\mathbf{r})$ is the mass density. The λ, μ and ρ are connected with the wave velocities in a medium through the relations $\mu = \rho c_t^2$ and $\lambda = \rho c_l^2 - 2\rho c_t^2$, where c_l and c_t are, respectively, the velocity of the longitudinal and the transverse component of the wave. In a multicomponent system the λ, μ and ρ are discontinuous functions of the position, $\mathbf{r}$.

As is mentioned above, here we study systems consisted of cylinders embedded in a homogeneous material. A cross section of such a system (periodic) is shown in Fig. 1. We consider the z axis parallel to the axis of the cylinders and propagation on the x-y plane. For such a system the parameters $\lambda(\mathbf{r})$, $\mu(\mathbf{r})$ and $\rho(\mathbf{r})$ do not depend on the coordinate z and the wave equation for the z component is decoupled from the equations for the x and the y component. The equations for the x and the y component can be written as

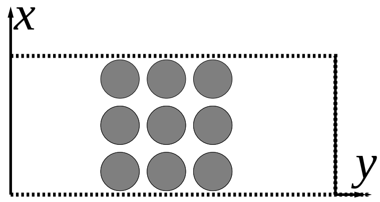

Figure 1. The computational cell.

$$\frac{\partial^2 u_x}{\partial t^2} = \frac{1}{\rho}(\frac{\partial T_{xx}}{\partial x} + \frac{\partial T_{xy}}{\partial y}), \quad (2)$$

$$\frac{\partial^2 u_y}{\partial t^2} = \frac{1}{\rho}(\frac{\partial T_{xy}}{\partial x} + \frac{\partial T_{yy}}{\partial y}), \quad (3)$$

where

$$T_{xx} = (\lambda + 2\mu)\frac{\partial u_x}{\partial x} + \lambda\frac{\partial u_y}{\partial y}, \quad T_{yy} = (\lambda + 2\mu)\frac{\partial u_y}{\partial y} + \lambda\frac{\partial u_x}{\partial x}, \quad (4)$$

$$T_{xy} = \mu(\frac{\partial u_x}{\partial y} + \frac{\partial u_y}{\partial x}). \quad (5)$$

The above equations consist the basis for the implementation of the FDTD in 2D systems. The computational domain for the calculations presented here is a rectangular area which contains a slab of the composite system in its central part (see Fig. 1). The sample is placed in a reservoir of the same material as the matrix material of the composite.

For the implementation of the FDTD method we divide the computational domain in $i_{\max} \times j_{\max}$ subdomains (grids) with dimensions $\Delta x, \Delta y$, and we define

$$u_\ell(i,j,k) = u_\ell(i\Delta x - \Delta x/2, j\Delta y - \Delta y/2, k\Delta t), \qquad \ell = x, y, \quad (6)$$

with $1 \le i \le i_{\max}$, $1 \le j \le j_{\max}$ and $k \ge 0$.

In the Eqs (2) - (5) we approximate the derivatives in both space and time with finite differences [21]. For the space derivatives we use central differences:

$$\begin{aligned} \frac{\partial u_\ell}{\partial x}|_{i,j,k} &\approx D_0^x u_\ell(i,j,k) = [u_\ell(i+1/2,j,k) - u_\ell(i-1/2,j,k)]/\Delta x, \\ \frac{\partial u_\ell}{\partial y}|_{i,j,k} &\approx D_0^y u_\ell(i,j,k) = [u_\ell(i,j+1/2,k) - u_\ell(i,j-1/2,k)]/\Delta y. \end{aligned} \quad (7)$$

For the time derivatives we use a combination of forward and backward differences:

$$\frac{\partial^2 u_\ell}{\partial t^2}|_{i,j,k} \approx D_+^t D_-^t u_\ell(i,j,k), \tag{8}$$

where

$$\begin{aligned} D_+^t u_\ell(i,j,k) &= [u_\ell(i,j,k+1) - u_\ell(i,j,k)]/\Delta t, \\ D_-^t u_\ell(i,j,k) &= [u_\ell(i,j,k) - u_\ell(i,j,k-1)]/\Delta t, \quad \ell = x, y. \end{aligned}$$

For Eq. (2), using expansion at (i,j,k) and following the procedure described above, we obtain

$$\begin{gathered} u_x(i,j,k+1) = 2u_x(i,j,k) - u_x(i,j,k-1) + \\ \frac{\Delta_t^2}{\rho(i,j)\Delta_x}[T_{xx}(i+1/2,j,k) - T_{xx}(i-1/2,j,k)] + \\ \frac{\Delta_t^2}{\rho(i,j)\Delta_y}[T_{xy}(i,j+1/2,k) - T_{xy}(i,j-1/2,k)]. \end{gathered} \tag{9}$$

For Eq. (3), expanding at $(i+1/2, j+1/2, k)$,

$$\begin{gathered} u_y(i+1/2,j+1/2,k+1) = \\ 2u_y(i+1/2,j+1/2,k) - u_y(i+1/2,j+1/2,k-1) + \\ \frac{\Delta_t^2}{\rho(i+1/2,j+1/2)\Delta_x}[T_{xy}(i+1,j+1/2,k) - T_{xy}(i,j+1/2,k)] + \\ \frac{\Delta_t^2}{\rho(i+1/2,j+1/2)\Delta_y}[T_{yy}(i+1/2,j+1,k) - T_{yy}(i+1/2,j,k)]. \end{gathered} \tag{10}$$

The T_{xx}, T_{xy}, T_{yy} are functions of the field components at the time $k\Delta t$, which are used for the updating of the fields for the next time. They are also discretized through Eqs (7) and their expressions after the discretization are given in the appendix A.

It has to be mentioned that the above way of discretization of the equations insures second order accurate central difference for the space derivatives. This has as a result, however, the field components u_x and u_y to be centered in different space points. To calculate, e.g., the field components $u_x(i+1/2, j+1/2, k)$, which are not stored in the computational memory, we use

$$\begin{aligned} u_x(i+1/2,j+1/2,k) = {} & [u_x(i+1,j+1,k) + u_x(i+1,j,k) + \\ & u_x(i,j+1,k) + u_x(i,j,k)+]/4. \end{aligned} \tag{11}$$

Using the above procedure the components u_x and u_y at the time step $k+1$ are calculated through their values at the step k. For insuring stability of the calculations we use the stability criterion [21]

$$\Delta t \leq 0.5/c\sqrt{1/\Delta x^2 + 1/\Delta y^2}, \tag{12}$$

where the velocity c is the highest among the sound velocities of the components of the composite.

The Δx and Δy are usually chosen as the 1/40 of the lattice constant (for periodic systems) with very big accuracy for waves with wavelength compared to the scatterers size.

In order to close the computational cell in the x-direction, for periodic or symmetric along the y-direction systems, we use periodic boundary conditions [$u(\mathbf{r}+\mathbf{R}) = \exp(i\mathbf{k}\cdot\mathbf{R})u(\mathbf{r})$ ($\mathbf{R}$: lattice vector)] along the y axis at $i=1$ and $i=i_{\rm max}$ (see dotted lines in Fig. 1). These conditions, here, can be expressed as

$$\mathbf{u}(i_{\rm max}+1, j, k) = \mathbf{u}(1, j, k), \tag{13}$$

$$\mathbf{u}(0, j, k) = \mathbf{u}(i_{\rm max}, j, k). \tag{14}$$

For closing the cell in the y-direction we use absorbing boundary conditions. In most of the cases the first order absorbing boundary conditions introduced by Zhou et. al. [20] have been used. These conditions are obtained by the requirement the reflection at the boundaries to be zero for two angles of incidence (θ_1, θ_2), and can be written in the form

$$A\frac{\partial \bar{\mathbf{u}}}{\partial x} + B\frac{\partial \bar{\mathbf{u}}}{\partial y} + I\frac{\partial \bar{\mathbf{u}}}{\partial t} = 0. \tag{15}$$

In Eq. (15) I is the identity 2×2 matrix, $\bar{\mathbf{u}}$ is the 2×1 matrix $[u_x, u_y]^T$ (T denotes the transpose of a matrix), and A, B are 2×2 matrices. For the boundary $j = j_{\rm max}$ the matrices A and B can be expressed as

$$A(\theta_1,\theta_2) = \frac{\eta_1}{\eta_1\xi_2 - \eta_2\xi_1}Q_2 - \frac{\eta_2}{\eta_1\xi_2 - \eta_2\xi_1}Q_1, \tag{16}$$

$$B(\theta_1,\theta_2) = \frac{\xi_2}{\eta_1\xi_2 - \eta_2\xi_1}Q_1 - \frac{\xi_1}{\eta_1\xi_2 - \eta_2\xi_1}Q_2, \tag{17}$$

with

$$Q_1 = \left[\begin{array}{cc} c_{lo}\xi_1^2 + c_{to}\eta_1^2 & (c_{lo}-c_{to})\xi_1\eta_1 \\ (c_{lo}-c_{to})\xi_1\eta_1 & c_{lo}\eta_1^2 + c_{to}\xi_1^2 \end{array}\right], \tag{18}$$

$$Q_2 = \left[\begin{array}{cc} c_{lo}\xi_2^2 + c_{to}\eta_2^2 & (c_{lo}-c_{to})\xi_2\eta_2 \\ (c_{lo}-c_{to})\xi_2\eta_2 & c_{lo}\eta_2^2 + c_{to}\xi_2^2 \end{array}\right], \tag{19}$$

and $\xi_i = \sin\theta_i$, $\eta_i = \cos\theta_i$ $(i = 1, 2)$. c_{lo} and c_{to} are, respectively, the longitudinal and the transverse wave velocity in the host material of the composite. For the boundary $j = j_{\min}$ the expressions of A and B are obtained from Eqs (16) and (17) by replacing θ_i by $\theta_i + \pi$ $(i = 1, 2)$. For the implementation of the condition (15) we require complete absorption for $\theta_1 = 0$ and $\theta_2 = \pi/4$

The condition (15) is discretized using central differences in space and forward differences in time:

$$\frac{\partial}{\partial t} \approx D_+^t, \quad \frac{\partial}{\partial x} \approx D_0^x \quad , \frac{\partial}{\partial y} \approx D_0^y. \tag{20}$$

For calculating the transmission we consider as incident wave a pulse with a Gaussian envelop in space. The pulse is formed at $t = 0$ in the left side of the composite and propagates along the y-direction. A longitudinal pulse like that has the form

$$u_y = \alpha \sin(\omega t - y/c_{lo}) \exp[-\beta(\omega t - y/c_{lo})^2], \tag{21}$$

while for a transverse one u_y is replaced by u_x and c_{lo} by c_{to}. The incident pulse is narrow enough in space as to permit the excitation of a wide range of frequencies.

The components of the displacement vector as a function of time are collected at various detection points depending on the structure of interest. They are converted into the frequency domain using fast Fourier transform. The transmission coefficient (T) is calculated either by normalizing the (frequency dependent) transmitted field amplitude $[(u_x^2+u_y^2)^{1/2}]$ by the incident field amplitude or through the energy flux vector $\mathbf{J}$ ($J_i = T_{ij} du_j/dt$). In the second case the transmitted flux vector is also normalized by the incident wave flux.

Concerning the case of pure acoustic waves (waves in fluid composites) the application of the FDTD starts again from the Eqs (2) - (5), but omitting the terms which include the Lamé coefficient μ. The equations are discretized through the same procedure as for the full elastic case. The boundary conditions coefficients are calculated again through the equations (16) - (19) where the velocity c_{to} must be replaced by c_{lo} (this replacement is essential in all the cases where the host material is fluid).

3. Results

In the present section we present results of the FDTD method for periodic systems and for systems with defects.

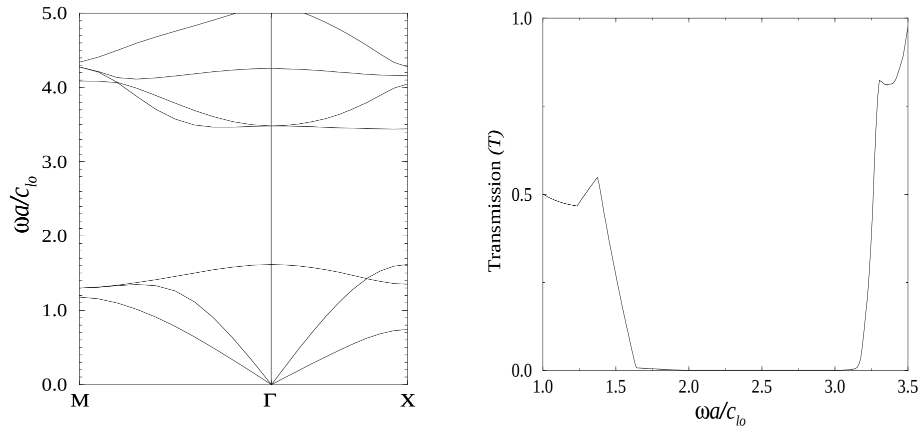

Figure 2. Left: Band structure along the MΓX direction for a periodic system of Cu cylinders in PMMA, in a square arrangement, with cylinder radius over lattice constant $r_c/a = 0.35$. The band structure is calculated through the PW method. c_{lo} is the longitudinal sound velocity in PMMA. Right: Transmission coefficient vs frequency for the system of the left panel. The incident wave is longitudinal propagating in the $< 10 >$ direction.

3.1. PERIODIC SYSTEMS

Using the FDTD method one can examine the existence of band gaps in a periodic composite system. This can be done by calculating the transmission coefficient through finite slabs of the system. Calculations like that provide a good test for the method as one can compare its results with corresponding results of other methods, where available. Here we calculate the transmission through a periodic composite consisting of Cu cylinders in PMMA host. We consider a 3×3 cylinders slab of the composite where the cylinders are placed within a square arrangement and the ratio of cylinder radius, r_c, over lattice constant, a, is 0.35. The result, which is shown in the right panel of Fig. 2, is compared with a corresponding result obtained through the PW method (see Fig. 2 - left panel). As one can see in Fig. 2, the agreement between the two methods is very good. Comparisons like that demonstrate the ability of the FDTD method to study the propagation in elastic multicomponent systems. It has to be mentioned, however, that the FDTD method is also able to calculate band structure (see Ref. [22] for such a calculation for EM waves), although through a more complicated procedure than that of the PW.

In Fig. 3 we compare FDTD results with results of a recent experimental study [11]. Fig. 3 shows the transmission coefficient for a periodic composite consisting of duraluminum cylinders in epoxy, in a square array,

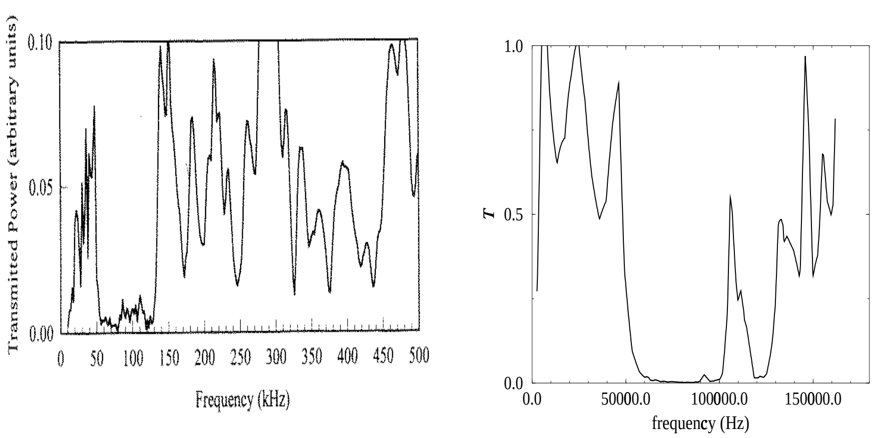

Figure 3. Left: Experimental transmission coefficient vs frequency for a system of duraluminum cylinders in epoxy (see Ref. [11]), in a square lattice, with cylinders radius over lattice constant $r_c/a = 0.4$. Right: Transmission coefficient, calculated trough the FDTD method, for the system of the left panel.

with $r_c/a = 0.4$. The left panel shows the experimental result and the right panel the corresponding FDTD result. The agreement between theory and experiment in the position and the width of the gaps is very good. The difference in the relative height of the peaks is due to the different size of the systems and due to the relatively high absorptivity of the epoxy, which has not been taken into account in the calculations.

3.2. DEFECTS

As we mentioned above, the FDTD method is ideal for the study of disorder induced phenomena. Here we exhibit this ability of the method by presenting results concerning systems with isolated defects.

We create an isolated defect by removing one cylinder from a periodic slab of the Cu in PMMA composite which was discussed in connection with Fig. 2. By removing one cylinder from a 3×3 cylinders slab of the composite and by calculating the transmission coefficient we obtain what is shown in the left panel of Fig. 4 - solid line (the dashed line shows the transmission for the periodic system). The transmission peak close to the midgap of the periodic system shows the formation of a defect state in this regime. Sending a monochromatic plane wave with the frequency of the defect state and examining the field over the sample we obtain the picture shown in the right panel of Fig. 4. The defect creates an s-like state, localized around the missing cylinder.

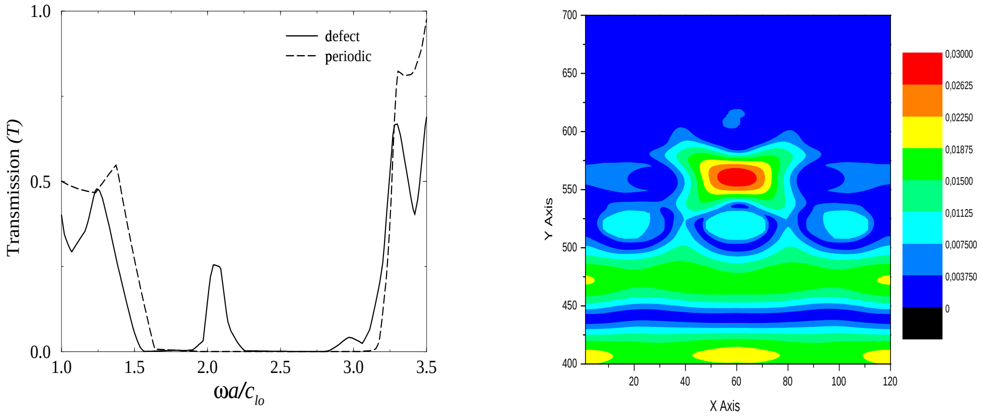

Figure 4. Left: Transmission coefficient vs frequency for a periodic system of Cu cylinders in PMMA, in a square arrangement, with cylinder radius over lattice constant $r_c/a = 0.35$, and with one missing cylinder (solid line) or without missing cylinder (dashed line). Right: The field over the sample for the system with the missing cylinder which discussed in the left panel. The incident wave is a a monochromatic plane wave with the frequency of the defect state.

3.3. WAVE GUIDES IN ELASTIC CRYSTALS

By removing a line of cylinders from a periodic composite instead of removing one single cylinder, one can create a linear defect. For electromagnetic wave propagation it has been shown [23, 24, 25] that such a defect can act as a waveguide for waves in the frequency regime of the gap as it consists the only channel of propagation for these waves. Recently, this guiding of waves through linear defects in periodic crystals was also shown for the case of the elastic waves [12, 26]. Using the FDTD method it was found that guides created as linear defects in elastic band gap materials can lead to total transmission of waves with frequency in the regime of the gap. The high transmitivity through such type of guides is demonstrated in the left panel of Fig. 5 (solid line). The results presented in Fig. 5 concern a 7×8 cylinders slab of a Cu in PMMA composite similar to the one of Fig. 2, from which we remove one row of cylinders. As one can see in Fig. 5, the transmission coefficient is close to one for almost all the gap regime of the periodic system. Sending monochromatic waves with frequencies in this regime ($T \approx 1$) one can see a great guiding of the waves through the defect state. This guiding is demonstrated in the right panel of Fig. 5, where it is shown the field created by a longitudinal incident plane wave with frequency the midgap frequency.

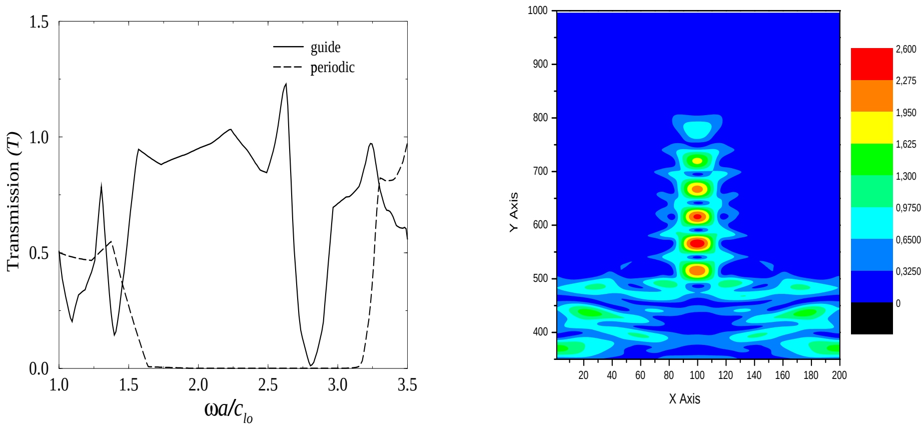

Figure 5. Left: Transmission coefficient vs frequency for a 7×8 cylinders slab of the Cu in PMMA composite discussed in Fig. 2, with one row of missing cylinders (solid line) or without missing cylinder (dashed line). Right: The field over the sample for the system of the left panel. The incident wave is a monochromatic plane wave at the midgap frequency.

Examining Fig. 5, however, one can see a pronounced dip in the transmission coefficient through the guide. Detailed examination of the origin of this dip (through band structure calculations) has shown that responsible for the dip is a gap in the propagation of the guided waves. The existence of gaps in the guided wave propagation (mini-gaps) is not something unexpected if one takes into account the periodic form of the guide "boundaries". These periodic "boundaries" impose a periodic potential in the guided wave propagation which, as the guided wave propagation is almost 1D, can easily lead to formation of gaps. The same "mini-gaps" possibly exist also for EM wave propagation through guides formed in photonic crystals, although such an existence has not been reported yet. The dips in the transmitivity of the guides formed as defects in elastic crystals is one of the main achievement of the FDTD in the field of elastic wave propagation in binary composites. Examination of the position of these dips showed that it depends on the material parameters of the components of the composites and mainly on the density and the velocities contrasts between scatterers and host.

4. Conclusions

We presented the FDTD method for 2D acoustic and elastic binary composites. The ability of the method to describe the wave propagation in these composites was demonstrated by presenting representative FDTD results for periodic systems (in comparison with PW and experimental results) and for single and line defects.

A. Calculation of the coefficients T_{xx}, T_{yy}, T_{xy}.

$$\begin{aligned} T_{xx}(i+1/2,j,k) = \\ (\lambda+2\mu)(i+1/2,j)[u_x(i+1,j,k)-u_x(i,j,k)]/\Delta_x + \\ \lambda(i+1/2,j)[u_y(i+1/2,j+1/2,k)-u_y(i+1/2,j-1/2,k)]/\Delta_y \end{aligned} \quad (22)$$

$$\begin{aligned} T_{xx}(i-1/2,j,k) = \\ (\lambda+2\mu)(i-1/2,j)[u_x(i,j,k)-u_x(i-1,j,k)]/\Delta_x + \\ \lambda(i-1/2,j)[u_y(i-1/2,j+1/2,k)-u_y(i-1/2,j-1/2,k)]/\Delta_y \end{aligned} \quad (23)$$

$$\begin{aligned} T_{xy}(i,j+1/2,k) = \\ \mu(i,j+1/2)[u_x(i,j+1,k)-u_x(i,j,k)]/\Delta_y + \\ \mu(i,j+1/2)[u_z(i+1/2,j+1/2,k)-u_y(i-1/2,j+1/2,k)]/\Delta_x \end{aligned} \quad (24)$$

$$\begin{aligned} T_{xy}(i,j-1/2,k) = \\ \mu(i,j-1/2)[u_x(i,j,k)-u_x(i,j-1,k)]/\Delta_z + \\ \mu(i,j-1/2)[u_y(i+1/2,j-1/2,k)-u_y(i-1/2,j-1/2,k)]/\Delta_x \end{aligned} \quad (25)$$

$$\begin{aligned} T_{xy}(i+1,j+1/2,k) = \\ \mu(i+1,j+1/2)[u_x(i+1,j+1,k)-u_x(i+1,j,k)]/\Delta_y + \\ \mu(i+1,j+1/2)[u_y(i+3/2,j+1/2,k)-u_y(i+1/2,j+1/2,k)]/\Delta_x \end{aligned} \quad (26)$$

$$\begin{aligned} T_{xy}(i,j+1/2,k) = \\ \mu(i,j+1/2)[u_x(i,j+1,k)-u_x(i,j,k)]/\Delta_y + \\ \mu(i,j+1/2)[u_y(i+1/2,j+1/2,k)-u_y(i-1/2,j+1/2,k)]/\Delta_x \end{aligned} \quad (27)$$

$$\begin{aligned} T_{yy}(i+1/2,j+1,k) = \\ (\lambda+2\mu)(i+1/2,j+1)[u_y(i+1/2,j+3/2,k) - \\ u_y(i+1/2,j+1/2,k)]/\Delta_y + \\ \lambda(i+1/2,j+1)[u_x(i+1,j+1,k)-u_x(i,j+1,k)]/\Delta_x \end{aligned} \quad (28)$$

$$\begin{aligned} T_{yy}(i+1/2,j,k) = \\ (\lambda+2\mu)(i+1/2,j)[u_y(i+1/2,j+1/2,k) - \\ u_y(i+1/2,j-1/2,k)]/\Delta_y + \\ \lambda(i+1/2,j)[u_x(i+1,j,k) - u_x(i,j,k)]/\Delta_x \end{aligned} \quad (29)$$

References

1. Soukoulis, C. M., ed. (1996) *Photonic Band Gap Materials,* Kluwer Academic Publishers.
2. Sigalas, M. M. & Economou, E. N. (1992) *J. Sound Vibration* **158**, 377; (1993) *Solid State Commun.* **86**, 141; (1994) *J. Applied Phys.* **75**, 2845; (1996) *Europhysics Lett.* **36**, 241.
3. Kushwaha, M. S., Halevi, P., Dobrzynski, L. & Djafari-Rouhani, B. (1993) *Phys. Rev. Lett.* **71**, 2022.
4. Economou, E. N. & Sigalas, M. M., in *Photonic Band Gaps and Localization* ed. by Soukoulis, C. M. (1993) Plenum Press, New York, pp. 317-338.
5. Economou, E. N. & Sigalas, M. M. (1993) *Phys. Rev.* B **48**, 13434; (1994) *J. Acoust. Soc. Am.* **95**, 1734.
6. Sigalas, M. M., Economou, E. N. & Kafesaki, M. (1994) *Phys. Rev. B* **50**, 3393.
7. Kafesaki, M., Sigalas, M. M. & Economou, E. N. (1995) *Solid State Commun.* **96**, 285.
8. Kushwaha, M. S. & Halevi, P. (1994) *Appl. Phys. Lett.* **64**, 1085; Kushwaha, M. S., Halevi, P, Martinez, G., Dobrzynski, L. & Djafari-Rouhani, B. (1994) *Phys. Rev.* B **49**, 2313.
9. Vasseur, J. O., Djafari-Rohani, B., Dobrzynski, L., Kushwaha, M. S. & Halevi, P. (1994) *J. Phys.:Condens. Matter* **6**, 8759.
10. Kushwaha, M. S. (1997) *Appl. Phys. Lett.* **70**, 3218.
11. Vasseur, J. O., Deymier, P. A., Frantziskonis, G., Hong, G., Djafari-Rohani, B., Dobrzynski, L. (1998) *J. Phys.:Condens. Matter* **10**, 6051.
12. Garcia-Pablos, D., Sigalas, M. M., Montero de Espinosa, F. R., Torres, M., Kafesaki, M. & Garcia, N. (2000) *Phys. Rev. Lett.* **84**, 4349.
13. Torres, M., Montero de Espinosa, F. R., Garcia-Pablos, D. & Garcia, N. (1998) *Phys. Rev. Lett.* **82**, 3054.
14. Montero de Espinosa, F. R., Jimenez, E. & Torres, M. (1998) *Phys. Rev. Lett.* **80**, 1208.
15. Martinez-Sala, R., Sancho, J., Sanchez, J. V., Gomez, V., Llinares, J. & Meseguer, F. (1995) *Nature* **378**, 241.
16. Kafesaki, M., Penciu, R. & Economou, E. N. (2000) *Phys. Rev. Lett.* **84**, 6050.
17. Kafesaki, M. & Economou, E. N. (1999) *Phys. Rev.* B **60**, 11993.
18. Smith, G.D., *Numerical Solution of Partial Differential Equations: Finite Difference Methods*, Claredon Press, Oxford.
19. Clayton, R. & Engquist, B. (1977) *Bull. Seism. Soc. Am.* **67**, 1529.
20. Zhou, J. & Saffari, N. (1996) *Proceedings of the Royal Society London*, Part A, **452**, 1609; (1997) *Bulletin of the Seismological Soc. of America* **87**, 1324.
21. Taflove, Allen (1995) *Computational Electrodynamics*, Artech House; Kunz, K. S. & Luebbers, R. J. (1993) *The finite difference time domain method for electromagnetics, CRC Press*; Jones, D. S. (1994) *Methods in electromagnetic wave propagation*, Oxford University Press.
22. Chan, C. T., Datta, S., Yu, Q. L., Sigalas, M. M., Ho, K. M. & Soukoulis, C. M. (1994) *Physica* **A211,** 411; Chan, C. T., Yu, Q. L. & Ho, K. M. (1995) *Phys. Rev.* B **51**, 16635.
23. Fan, S., Villeneuve, P. R. & Joannopoulos, J. D. (1996) *Phys. Rev.* B **54**, 11245.

24. Mekis, A., Chen, J. C., Kurland, I., Fan, S., Villeneuve, P. R. & Joannopoulos, J. D. (1996) *Phys. Rev. Lett.* **77**, 3787.
25. Sigalas, M. M., Biswas, R., Ho, K. M., Soukoulis, C. M. & Crouch, D. D. (1999) *Phys. Rev.* B **60**, 4426.
26. Kafesaki, M., Sigalas, M. M. & Garcia, N. (2000) to appear in *Phys. Rev. Lett.*
27. Landau, L. D. & Lifshitz, E. M. (1959) *Theory of Elasticity*, Pergamon.